# Inorganic Chemistry © Cite This: Inorg. Chem. 2019, 58, 16553–16558

pubs.acs.org/IC

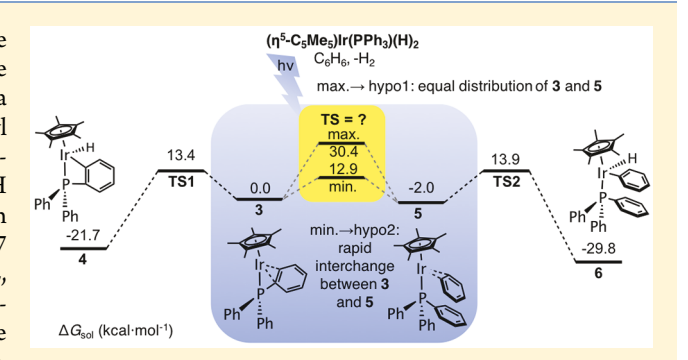
# Theoretical Analysis of Competing Pathways for Carbon-Hydrogen Activation of Cyclopentadienyl-Triphenylphosphine-Iridium in Benzene

Xin Yang<sup>®</sup> and Michael B. Hall\*<sup>®</sup>

Department of Chemistry, Texas A&M University, College Station, Texas 77845, United States

Supporting Information

**ABSTRACT:** Density functional theory (DFT) calculations are used to evaluate alternative reaction mechanisms when the photochemically produced ( $\eta^5$ -C<sub>5</sub>Me<sub>5</sub>)IrPPh<sub>3</sub> oxidatively adds a C-H bond from either a benzene solvent molecule or a phenyl group of the phosphine ligand. Experimentally, the orthometalated complexes produced from intramolecular C-H activation and the hydridophenyl complexes produced from intermolecular C-H activation form in a ratio of 53:47 (Janowicz, A. H.; Bergman, R. G. J. Am. Chem. Soc. 1982, 104, 352-354). Both products are predicted to be thermodynamically stable such that the back reaction, reductive elimination, is predicted to be exceedingly unfavorable. Thus,



the product ratio must be under kinetic control. The DFT calculations predict the initial formation of  $\pi$ -bound intermediates,  $\eta^2$ -C<sub>6</sub>H<sub>5</sub>X (X = H or PPh<sub>2</sub>), with the intermolecular  $\pi$ -intermediate 2.0 kcal/mol more stable in free energy than the intramolecular  $\pi$ -intermediate. From these intermediates, the two competing reactions have slightly different free-energy barriers. The intramolecular activation of a phenyl C-H bond to yield ortho-metalated complexes has a barrier of 13.4 kcal/ mol, and the intermolecular oxidative addition of solvent molecule C<sub>6</sub>H<sub>6</sub> to form (η<sup>5</sup>-C<sub>5</sub>Me<sub>5</sub>)Ir(PPh<sub>3</sub>)(Ph)H has a barrier of 15.9 kcal/mol. We propose that exchange between the  $\pi$ -intermediates is faster than the oxidative additions, so the dominant early intermediate is the intermolecular  $\pi$ -intermediate. Hence, from this intermediate the two reaction paths have free-energy barriers of 15.4 (intramolecular) and 15.9 (intermolecular) kcal/mol. Thus, within the accuracy of DFT, the free-energy barriers for the intramolecular pathway and the intermolecular pathway are very compatible with the 53:47 product ratio. However, the calculations cannot completely exclude a higher interchange barrier, which would mean that the final product ratio must result from the nearly equal distribution (53:47) of the two  $\pi$ -intermediates that then proceed toward their own products. Further calculations on the less sterically crowded ( $\eta^{5}$ -C<sub>5</sub>H<sub>5</sub>)IrPPh<sub>3</sub> predict that the intermolecular product should dominate the ratio.

## **■ INTRODUCTION**

Inspired by the prevalence of photochemical reactions in nature, such as photosynthesis, bioluminescence, and vision, research in photochemistry has received much attention because of its potential in utilizing light as a source of energy. 1-6 Many transition-metal complexes are photoactive and capable of triggering a cascade of reactions because of long-lived excited states and appropriate energy gaps between ground states and lowest excited states. They offer the possibility to initiate reactions photochemically at low temperature and provide alternative routes for synthesis. Among photoactive transition-metal complexes, metal hydrides have played a critical role in the carbon-hydrogen bond activation of arenes and alkanes, hydrogen evolution crosscoupling, and other C-H functionalization reactions.

The loss of  $H_2$  or CO from transition-metal complexes is one of the most common photochemical pathways to the activation of other  $\sigma$  bonds, especially C-H bonds. In 1972, Green and collaborators reported that the photolysis of  $Cp_2W(H)_2$  ( $Cp = \eta^5 - C_5H_5$ ) in solution induced the reductive

elimination of H<sub>2</sub> and the insertion of [Cp<sub>2</sub>W] into aromatic C-H bonds. 10 In the 1980s, several groups began investigations to achieve direct, one-stage intermolecular oxidative addition to saturated hydrocarbons. Graham et al. reported the stoichiometric oxidative addition of carbon-hydrogen bonds of neopentane and cyclohexane to a photochemically generated iridium complex from  $(\eta^5-C_5Me_5)Ir(CO)_2$ . They presumed that the 16-electron iridium(I) intermediate ( $\eta^{5}$ -C<sub>5</sub>Me<sub>5</sub>)Ir(CO) was produced upon irradiation, to which the carbon-hydrogen bonds of benzene, neopentane, and cyclohexane oxidatively added. At almost the same time, Bergman et al. discovered a closely related system  $(\eta^5-C_5Me_5)Ir(PMe_3)$ -(H)<sub>2</sub>, which went through the photodissociation of H<sub>2</sub> and the formation of  $(\eta^5 - C_5 Me_5) Ir^{III}(H)(R)(PMe_3)(R = phenyl,$ neopentyl, cyclohexyl) as a result of C-H bond activation. The wide-ranging experimental works on this subject were extensively reviewed. <sup>14–16</sup> In addition, computational studies

Received: August 27, 2019 Published: November 25, 2019



Scheme 1. Schematic Representation of C-H Activation by (η<sup>5</sup>-C<sub>5</sub>Me<sub>5</sub>)Ir(PPh<sub>3</sub>)(H)<sub>2</sub>

$$(\eta^5\text{-}C_5\text{Me}_5)\text{Ir}(\text{PPh}_3)(\text{H})_2 \xrightarrow[\text{hv}]{} (\eta^5\text{-}C_5\text{Me}_5)(\text{PPh}_3)\text{Ir} \xrightarrow[\text{Ph}_2\text{P}]{} + (\eta^5\text{-}C_5\text{Me}_5)\text{Ir}$$

also advanced our understanding of how transition-metal complexes catalyze C-H activation reactions. Detailed descriptions can be found in the reviews by Hall, Eisenstein, and co-workers. 17,18 Our group has a long-standing interest in understanding the kinetics of C-H activation in Cp'ML (Cp' =  $\eta^5$ -C<sub>5</sub>H<sub>5</sub> or  $\eta^5$ -C<sub>5</sub>Me<sub>5</sub>, M = Rh, Ir) complexes. Our previous study in collaboration with M. W. George showed that lifetime variations in the Cp'Rh(CO)(alkane) system were a reflection of the subtle interplay between the rates of activation and migration. 19,20 Pitts et al. later extended the study to cycloalkanes and found that compared to linear alkanes the migration barriers were lower and the activation barriers were higher for larger rings, increasing the lifetime of  $\sigma$ -complexes and influencing the overall rate of C-H activation, showing an unexpectedly dramatic change between cyclohexane and cycloheptane.<sup>21</sup> Parallel studies on TpRh complexes have also been reported.<sup>22,23</sup>

One of the common features of classical photoinitiated C-H activation studies is that the reactions typically proceed in pure solvent as the reactant. The intermolecular selectivity of C-H bonds can be determined from product ratios by using mixtures of two hydrocarbons as solvent. Rare are cases that involve both intramolecular and intermolecular C-H activation, which makes the reaction in Scheme 1 particularly interesting, where the extrusion of dihydrogen was detected when  $(\eta^5-C_5Me_5)Ir(PPh_3)(H)_2$  was irradiated in benzene, followed by the activation of both intramolecular and intermolecular C-H bonds. The ortho-metalated complex and the hydridophenyl complex formed in a 53:47 ratio.<sup>13</sup> Irradiation in a solvent of acetonitrile gave all ortho-metalated products. When CpIr(PMe<sub>3</sub>)(H)<sub>2</sub> was used for irradiation in benzene, only the hydridophenyliridium complex was obtained. Because of limitations in methodologies and techniques available at the time, not much information was provided about the dynamics of the reaction. Although timeresolved experiments were found for closely related carbonyl analogues  $Cp'M(CO)_2(M = Rh \text{ or Ir})$  with hydrocarbons, comparative studies for LM(PPh<sub>3</sub>) reactants in hydrocarbons have been neglected, in part because they lack the conveniently measured CO ligands. 24-26

In this work, the photochemical reaction of  $(\eta^5 - C_5 Me_5)$  Ir- $(PPh_3)(H)_2$  in benzene (Scheme 1) is reinvestigated from a theoretical perspective using density functional theory. This study is aimed at understanding the experimentally observed product ratio (ortho-metalated complexes/hydridophenyl complexes = 53:47), where the enthalpically favored intermolecular products are formed in a ratio nearly equal to that of the entropically favorable intramolecular products. The mechanisms are calculated in an attempt to understand the competing intra- and intermolecular formation processes. The interchange routes between the two pathways and other factors such as solvent effects and concentration differences that could shift activation energies and the chemical equilibrium are also investigated.

#### ■ COMPUTATIONAL METHODS

All theoretical calculations were performed with Gaussian 09, revision D01.<sup>27</sup> Calculations from coupled cluster theory, CCSD(T), were used to benchmark a variety of functionals: TPSS, <sup>28</sup> M11, <sup>29</sup> M11-L, <sup>30</sup> MN12SX,<sup>31</sup> and ωB97XD.<sup>32</sup> In these benchmark calculations, truncated molecular models CpIr(PH2Ph) and CpIr(PH3) were used for the intra- and the intermolecular reactions, respectively (Scheme S1). The geometries used for CCSD(T) calculations were optimized from the TPSS functional in combination with basis set BS1 (aug-cc-pVQZ-pp<sup>33</sup> for Ir with the corresponding pseudopotential and cc-pVTZ<sup>34</sup> for C, H, and P). The electronic energies obtained from single-point CCSD(T) calculations using BS2 (cc-pVTZ-pp for Ir with the corresponding pseudopotential and cc-pVTZ for C, H, and P) were corrected to the complete basis set (CBS) limit. This basisset extrapolation was based on a series of MP2 calculations with systematic increases in the basis set (cc-pVTZ, cc-pVQZ, and ccpV5Z) (Tables S3-S8). The activation energy was calculated to be 26.30 kcal/mol for the intermolecular reaction and 16.55 kcal/mol for the intramolecular reaction at the CBS limit (Table S1). Because the major concern was the relative rate between the intermolecular and intramolecular reaction, the 9.75 kcal/mol activation energy difference was used to evaluate the performance of density functionals for this system. Each species presented in CCSD(T) calculations was optimized by the tested functionals mentioned above using BS2. M11 was selected because it produced an activation energy difference (9.85 kcal/mol) closest to the benchmark value among the tested functionals. Optimization and frequency calculations were performed on full molecular models at M11/BS2. Solvent corrections to free energies have been made through single-point calculations on gasphase-optimized geometries using the SMD model.<sup>35</sup> For an association reaction  $A + B \rightarrow C$ , the computed Gibbs free energies  $(G_{atm}^{\circ})$ , which correspond to a 1 atm standard state, were corrected to a 1 M solution standard state  $(G_{M}^{\circ})$ , and a standard state correction was applied ( $\Delta G^{\circ}_{M} = \Delta G^{\circ}_{atm} - 1.9$  kcal/mol, Section S3 in the SI). Because the intermolecular reaction has the solvent as a reactant, the large benzene to Ir complex ratio results in drastically different effective concentrations for intra- and intermolecular reactions. To compare the rate of the intra- and intermolecular reactions on the same scale, a concentration correction (-5.1 kcal/)mol, Section S3 in the SI) to the Gibbs free energy was further applied to species in the intermolecular pathway.

#### RESULTS

Intramolecular Reaction. The energy profile for the ortho-metalation pathway of  $(\eta^5-C_5Me_5)$ IrPPh<sub>3</sub> is shown in Scheme 2. As expected, the phenyl groups in the propeller-like PPh<sub>3</sub> ligand are not symmetric in these complexes and are arranged in such a way as to minimize the ring-ligand interaction and ring-ring repulsion in the pseudo-octahedral complexes.<sup>36</sup> Reactant dihydride complex 1 is fully optimized (Figure S1) in order to compare energetic and geometric changes with other species involved in the reaction. Losing a dihydride from complex 1 followed by geometry optimization results in a  $16e^-$  Ir( $\bar{I}$ ) complex that is optimized to a stationary point on the potential energy surface with no imaginary frequencies, which is labeled as complex 2 (Scheme 2 and Figure 1). The C-H bond closest to Ir in complex 2 (labeled C<sub>2</sub>-H) is slightly longer (1.090 Å) than other C-H bonds (1.084-1.086 Å) on the same phenyl ring, indicating weak  $\sigma$ interaction with the metal center. This weak  $\sigma$ -complex, 2, is

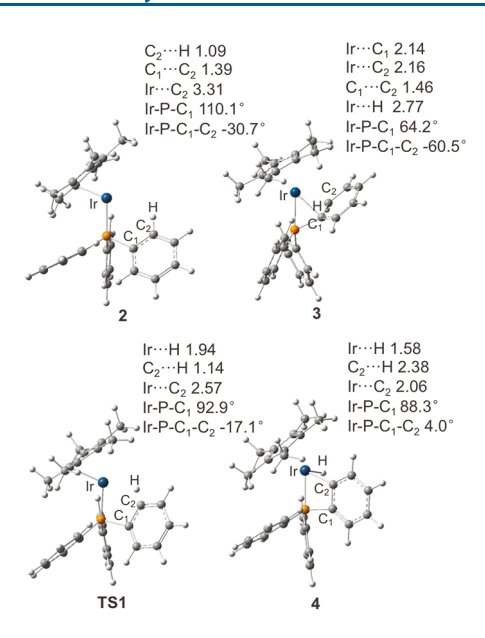


**Figure 1.** Optimized geometric structures of selected species along the intramolecular reaction pathway. Bond distances are shown in angstroms.

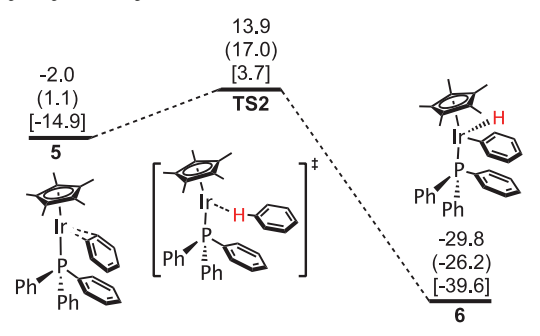
unstable with TPSS or  $\omega$ B97XD functionals, and their geometry optimizations lead directly to intermediate 3. Intermediate 3 could be obtained by all other tested functionals and is found to be 9.6 kcal/mol more stable than isomer 2 with the M11 functional. Hence, complex 3 is set to zero for all energy profiles. In complex 3, two Ir-C<sub>phenyl</sub> distances were shortened to 2.14 and 2.16 Å and then the C<sub>1</sub>-C<sub>2</sub> double bond was stretched to 1.46 Å (1.39 Å in complexes 1 and 2), suggesting the formation of an intramolecular  $\pi$ -complex. This distortion is accompanied by a decrease in the  $Ir-P-C_1-C_2$  dihedral angle (from -30.7 in 2 to  $-60.5^{\circ}$  in 3) and a decrease in the Ir-P-C<sub>1</sub> angle (from 110.1 in 2 to  $64.2^{\circ}$  in 3). The search for a transition state between 2 and 3 produced one which is 1.5 kcal/mol above 2 in free energy with an extremely small imaginary frequency (f = 19.06i), corresponding to the motion of decreasing the Ir-P-C angle (Figure S2).

Next, the oxidative addition reaction of the intramolecular phenyl C-H bond proceeded via transition state **TS1**. In **TS1**, the H being activated was nearly coplanar with Ir-P-C<sub>1</sub>, the

Ir-P- $C_1$ - $C_2$  dihedral angle increased from  $-60.2^{\circ}$  in 3 to -17.1° in TS1, and the Ir-P-C<sub>1</sub> angle increased to 92.9° in TS1. The Ir-H distance shortened to 1.94 Å, and the C-H bond elongated to 1.14 Å. The single imaginary frequency (71.1i) of TS1 corresponds to the Ir-H distance change coupled to the phenyl ring rotation around the P-C<sub>1</sub> bond and the P-C<sub>1</sub>-C<sub>2</sub> angle change. Such a motion enabled the activated C and H atoms to approach Ir, cleaving the C-H bond and forming new Ir-H and Ir-C bonds. TS1 was 3.8 kcal/mol higher in free energy than intermediate 2 and 13.4 kcal/mol higher than intermediate 3. In newly formed product 4, the Ir-H and Ir-C<sub>2</sub> bond lengths were 1.58 and 2.06 Å, respectively. Product 4 was 35.1 kcal/mol more stable than TS1. In summary, a free-energy barrier of 13.4 kcal/mol is predicted for the formation of ortho-metalated product 4 from 3 via the intramolecular pathway.

**Intermolecular Reaction.** Activating a free benzene molecule with the Ir photoproduct requires two general steps: association and then activation. Association of the solvent benzene with the electron-deficient  $(\eta^5 - C_5 Me_5)$ IrPPh<sub>3</sub> fragment yields  $\eta^2$ - $\pi$ -complex 5 (Scheme 3, Figure 2).

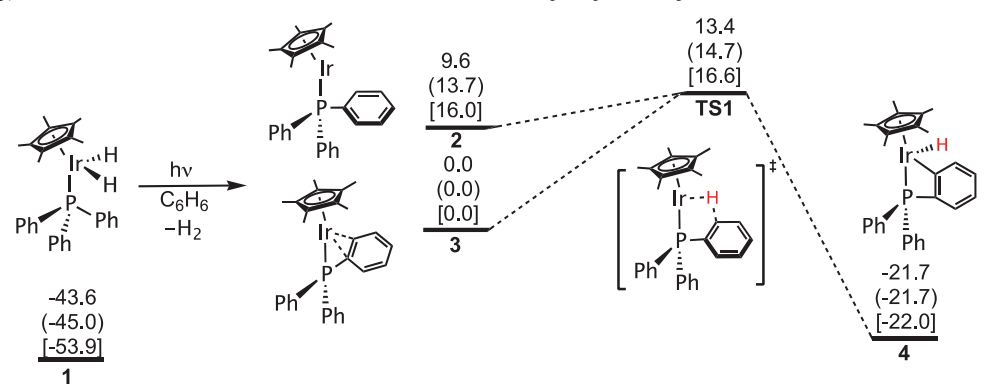
Scheme 3. Energy Profile for the Intermolecular Reaction of  $(\eta^5-C_5Me_5)$ IrPPh<sub>3</sub> with Benzene<sup>a</sup>



"Relative free energies in solvent, free energies in the gas phase (in parentheses), and enthalpies in the gas phase [in square brackets] in kcal/mol are shown.

Experimental evidence for the intermediacy of an  $\eta^2$ -arene complex in the activation of aromatic C–H bonds was observed by Jones for the  $(\eta^5\text{-}C_5\text{Me}_5)\text{Rh}[\text{PMe}_3](\text{H})(\text{C}_6\text{H}_5)$  complex early in 1982.<sup>37</sup> Natural bond orbital (NBO) analysis was also performed to scrutinize this type of coordination in

Scheme 2. Energy Profile for the Intramolecular Reaction of  $(\eta^5-C_5Me_5)$ IrPPh<sub>3</sub><sup>a</sup>



<sup>&</sup>quot;Relative free energies in solvent, free energies in the gas phase (in parentheses), and enthalpies in the gas phase [in square brackets] in kcal/mol are shown.

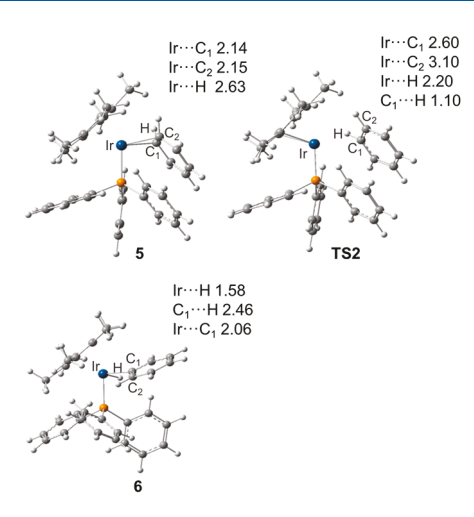
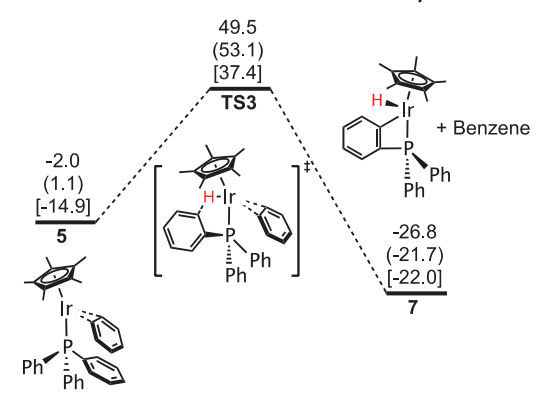


**Figure 2.** Optimized geometric structures of selected species along the intermolecular reaction pathway. Bond distances are shown in angstroms.

structurally related complexes.<sup>38</sup> Interestingly, the lengths of the Ir- $C_1$  bond and the lengths of the  $\eta^2$ -coordinated  $C_1$ - $C_2$ double bond in 5 were almost the same as those in intramolecular  $\pi$ -complex 2. As shown in Figure 2, the coordinated benzene in complex 5 is parallel but displaced from a phenyl ring on the phosphine, so it appears to be stabilized by  $\pi - \pi$  stacking. Complex 5 is enthalpically more stable than 3 by 14.9 kcal/mol but only 2.0 kcal/mol more stable in free energy because of the entropy loss. The next step is the oxidative addition of a benzene C-H bond to form the new Ir-C and Ir-H bonds. In spite of numerous searches, a stable  $\sigma$ -complex was not formed before the association of benzene in forming  $\pi$ -complex 5 or between  $\pi$ -complex 5 and the oxidative-addition transition state, TS2 (imaginary frequency = 113.6i). From 5 to TS2, the Ir-C distances changed from 2.14 and 2.15 to 2.60 and 3.10 Å, and the Ir-H distance shortened to 2.20 Å and the C<sub>1</sub>-H length slightly elongated to 1.10 Å. The Gibbs free energy barrier from 5 to TS2 was calculated to be 15.9 kcal/mol. The Ir-H and Ir-C<sub>1</sub> bond lengths in intermolecular oxidative-addition product 6 (Figure 2) are similar to those in intramolecular product 4. Compared to the intramolecular reaction's enthalpy ( $\Delta H =$ -22.0 kcal/mol), the intermolecular reaction is more exothermic ( $\Delta H = -39.6 \text{ kcal/mol}$ ). In spite of the large enthalpy difference, hydridophenyl product 6 is only 8.1 kcal/ mol lower in free energy than ortho-metalated product 4, again a reflection of entropy and concentration differences.

**Interchange.** As shown in Scheme 4, ortho-metalated product 7 could also be produced from complex 5 via a intramolecular oxidative-addition interchange path through transition state **TS3**. **TS3** has an imaginary vibrational frequency of 646 cm<sup>-1</sup>, corresponding to the movement of the H between the phosphine phenyl carbon and the Ir, with selected geometric features shown in Figure 3. Compared to  $\pi$ -complex intermediate 5, the Ir–C distances for the benzene in **TS3** are almost the same (2.15 and 2.18 Å), indicating that  $\pi$ -coordination is not affected by the C–H activation. The Ir–H length in **TS3** was much shorter (1.63 Å) and the C<sub>3</sub>–H bond was longer (1.40 Å) than those in **TS1** and **TS2**. Although the C<sub>5</sub>Me<sub>5</sub> tilts away to reduce the increasing electron density in the transition state, it did not bring the barrier (51.5 kcal/mol above **5**) into a viable range. We hypothesized that the higher

Scheme 4. Energy Profile for the Interchange of the Intermolecular and Intramolecular Pathways<sup>a</sup>



"Relative free energies in solvent, free energies in the gas phase (in parentheses), and enthalpies in the gas phase [in square brackets] in kcal/mol are shown.

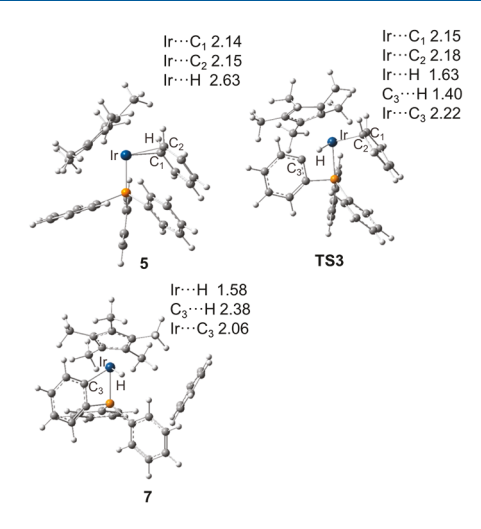


**Figure 3.** Optimized geometric structures of selected species along the intramolecular reaction pathway. Bond distances are shown in angstroms.

relative free energy of transition state TS3 came from the complex's reluctance to accept two more electrons and become a nearly  $20e^-$  transition state. As the formation of the new Ir—H and Ir— $C_3$  bonds are completed, the  $\eta^2$ -benzene dissociates and drifts away. The reaction path shown in Scheme 4 produces ortho-metalated product 7, in this orientation as the optical isomer of 4 in Scheme 3.

## DISCUSSION

The reverse reaction, reductive elimination, from the intra- and intermolecular products, 4 and 6, would need to proceed back over TS1 and TS2 with free-energy barriers of 35.1 and 43.7 kcal/mol, respectively. Thus, from the high reverse barriers, we conclude that the reaction is under kinetic control.

The results shown in Scheme 4 indicates that a concerted interchange between the inter- and intramolecular pathways from 5 to 7 is excluded because of the high barrier at TS3, and an alternative interchange could occur between intermolecular  $\pi$ -complex 5 and intramolecular  $\pi$ -complex 3. Unfortunately, our extensive search for such a concerted barrier between 5 and 3 led to the dissociation of the PPh<sub>3</sub> ligand. Because such

concerted interchanges all involve 20-electron transition states, they will have high barriers or will result in the dissociation of another ligand. Thus, the only possibility of an interchange between the two pathways would be through a species such as 2. For this situation, the upper limit for the free-energy barrier in the simple dissociation of a benzene from 5 to form 2 can be estimated as the enthalpy of dissociation, (14.9 (3-5) + 16.0 (2-3) = 30.9 kcal/mol), which is substantially higher than the oxidative-addition barriers. Thus, in this situation the final product distribution would be totally dependent on the initial distribution of the  $\pi$ -intermediates, which must be almost equal in order to explain the observed product distribution.

However, our calculation shows that a subtle geometry displacement of species 2 leads to 3, which might indicate that the interchange barrier between 5 and 3 is substantially overestimated above. If the free-energy barrier between 5 and 3 is estimated at its lower limit, it would involve just the enthalpic difference (3-5 = 14.9 kcal/mol). In the reverse direction from 3 to 5, the lower limit would be the free-energy barrier between 3 and 2 plus the attachment barrier for a benzene molecule to enter the iridium's coordination sphere  $(9.6 (3-2) + \sim 3.3) = 12.9 \text{ kcal/mol}$ . These two estimates produce a consistent barrier with both directions. Although the value of 3.3 was chosen to produce consistent barriers for both directions, such a value is also consistent with the measured lifetime for the coordination of species following photochemical ligand ejection. 21,23 With this barrier, which is smaller than either of the C-H activation free-energy barriers, intermolecular  $\pi$ -intermediate 5 would predominate initially in the reaction mixture after the photolysis because of its lower free energy. Then, it would cost 15.9 kcal/mol for 5 to reach TS2 (2.0 + 13.9) on the intermolecular pathway, and it would cost 15.4 kcal/mol for 5 to reach TS1 via 3 (2.0 + 13.4 on the intramolecular pathway). Therefore, these calculated barriers are highly consistent with the experimental findings that the intra- and intermolecular products, 4 and 6, are present in a ratio of 53:47.

To compare electronic vs steric effects, we calculated the energetics of the Cp-substituted analogues,  $(\eta^5-C_5H_5)$ IrPPh<sub>3</sub> (Scheme S5 in SI). Despite the fact the Cp is a poorer donor compared to  $\eta^5$ -C<sub>5</sub>Me<sub>5</sub>, the barriers for both the intra- and intermolecular activation steps are lower (Scheme S5). For  $(\eta^5-C_5H_5)$ IrPPh<sub>3</sub>, the intra- and intermolecular free-energy barriers with respect to their intermediates are 12.8 and 13.6 kcal/mol, respectively, and for  $(\eta^5-C_5Me_5)$ IrPPh<sub>3</sub> they are 13.4 and 15.9 kcal/mol. Interestingly, for the  $(\eta^5-C_5H_5)$ IrPPh<sub>3</sub> system the intermolecular intermediate,  $\eta^2$ - $\pi$ -complex 5'', is 4.8 kcal/mol more stable than the corresponding intramolecular intermediate, 3", whereas for the  $(\eta^5-C_5Me_5)$ IrPPh<sub>3</sub> system, 5 is only 2.0 kcal/mol more stable than 3. Applying the pre-equilibrium argument described above raises the barrier for the intramolecular path by 4.8 kcal/mol, which raises the intramolecular free-energy barrier to 17.6 kcal/mol, much higher than the intermolecular free-energy barrier of 13.6 kcal/ mol (Scheme S5). Thus, for these C-H activations the steric effect of Cp outweighs its electronic effect, especially in the intermolecular reaction that has a lower activation energy and a more stable intermediate, which raises the effective activation barrier for the intramolecular reaction. Experimentally, the predicted ratio would be much closer to 1:99. From the alternative perspective, the bulky  $\eta^5$ -C<sub>5</sub>Me<sub>5</sub> slows down the intermolecular C-H activation substantially more than the intramolecular one.

#### CONCLUSIONS

The geometries, electronic structures, and energetics of the Ir complexes in the photochemical reaction of  $(\eta^5-C_5Me_5)$ Ir-(PPh<sub>3</sub>)(H)<sub>2</sub> in benzene were studied by DFT calculations. The DFT electronic energy barriers for the oxidative addition of a C-H bond from PPh3 and that of benzene were calibrated against CCSD(T) calculations, which resulted in our choice of M11 for this study. Extensive analysis of the results provide two alternate explanations for the experimental ratio (53:47) of the two products (intra-/intermolecular). If the two pathways rapidly interchange before oxidative addition, then the freeenergy barrier for the intermolecular reaction that generate the hydridophenyl complex is 15.9 kcal/mol, while that for the intramolecular reaction that generates the ortho-metalated product is 15.4 kcal/mol. The intramolecular barrier is 0.5 kcal/mol lower than the intermolecular barrier, indicating that the ortho-metalated complexes should be slightly more favored. This conclusion successfully justifies the product ratio reported in the experiment. However, we cannot exclude the possibility that the interchange barrier between the intraand intermolecular  $\pi$ -intermediates is higher than the oxidative-addition barriers. In this case, the observed product distribution must result from nearly equal initial distributions of the  $\pi$ -intermediates after the photolysis. Finally, the calculations on less sterically crowded ( $\eta^5$ -C<sub>5</sub>H<sub>5</sub>)IrPPh<sub>3</sub> predict that similar experiments on this system would produce significantly different ratios if the pre-equilibrium argument is correct.

#### ASSOCIATED CONTENT

# Supporting Information

The Supporting Information is available free of charge at https://pubs.acs.org/doi/10.1021/acs.inorgchem.9b02580.

Computational details (PDF) Cartesian coordinates (ZIP)

#### AUTHOR INFORMATION

# **Corresponding Author**

\*E-mail: mbhall@tamu.edu.

ORCID ®

Xin Yang: 0000-0003-0085-7859 Michael B. Hall: 0000-0003-3263-3219

Notes

The authors declare no competing financial interest.

# ACKNOWLEDGMENTS

We are grateful for financial support from the National Science Foundation (CHE-1664866) and the Robert A. Welch Foundation (A-0648). The authors acknowledge the Laboratory for Molecular Simulation (https://lms.chem.tamu.edu) and the High Performance Research Computing Facility (http://hprc.tamu.edu) for providing computing resources useful in conducting the research reported in this article.

#### REFERENCES

- (1) Wenger, O. S. Photoactive Complexes with Earth-Abundant Metals. *J. Am. Chem. Soc.* **2018**, *140*, 13522.
- (2) Chen, B.; Wu, L.-Z.; Tung, C.-H. Photocatalytic Activation of Less Reactive Bonds and Their Functionalization via Hydrogen-Evolution Cross-Couplings. *Acc. Chem. Res.* **2018**, *51*, 2512.
- (3) Perutz, R. N.; Procacci, B. Photochemistry of Transition Metal Hydrides. *Chem. Rev.* **2016**, *116* (15), 8506–8544.

- (4) Stoll, T.; Castillo, C. E.; Kayanuma, M.; Sandroni, M.; Daniel, C.; Odobel, F.; Fortage, J.; Collomb, M.-N. Photo-Induced Redox Catalysis for Proton Reduction to Hydrogen with Homogeneous Molecular Systems Using Rhodium-Based Catalysts. *Coord. Chem. Rev.* 2015, 304–305, 20–37.
- (5) Artero, V.; Chavarot-Kerlidou, M.; Fontecave, M. Splitting Water with Cobalt. *Angew. Chem., Int. Ed.* **2011**, *50* (32), 7238–7266. (6) Esswein, A. J.; Nocera, D. G. Hydrogen Production by Molecular
- Photocatalysis. Chem. Rev. 2007, 107 (10), 4022–4047.
- (7) Arndtsen, B. A.; Bergman, R. G.; Mobley, T. A.; Peterson, T. H. Selective Intermolecular Carbon-Hydrogen Bond Activation by Synthetic Metal Complexes in Homogeneous Solution. *Acc. Chem. Res.* 1995, 28 (3), 154–162.
- (8) Jones, W. D.; Feher, F. J. Comparative Reactivities of Hydrocarbon Carbon-Hydrogen Bonds with a Transition-Metal Complex. *Acc. Chem. Res.* **1989**, 22 (3), 91–100.
- (9) Jones, W. D. Isotope Effects in C-H Bond Activation Reactions by Transition Metals. *Acc. Chem. Res.* **2003**, *36* (2), 140–146.
- (10) Giannotti, C.; Green, M. L. H. Photo-Induced Insertion of Bis $\pi$ -Cyclopentadienyltungsten into Aromatic Carbon—Hydrogen Bonds. *J. Chem. Soc., Chem. Commun.* **1972**, No. 20, 1114b—11115.
- (11) Hoyano, J. K.; Graham, W. A. G. Oxidative Addition of the Carbon-Hydrogen Bonds of Neopentane and Cyclohexane to a Photochemically Generated Iridium(I) Complex. J. Am. Chem. Soc. 1982, 104 (13), 3723–3725.
- (12) Janowicz, A. H.; Bergman, R. G. Activation of Carbon-Hydrogen Bonds in Saturated Hydrocarbons on Photolysis of (. Eta. 5-C5Me5)(PMe3)IrH2. Relative Rates of Reaction of the Intermediate with Different Types of Carbon-Hydrogen Bonds and Functionalization of the Metal-Bound Alkyl Groups. *J. Am. Chem. Soc.* 1983, 105 (12), 3929–3939.
- (13) Janowicz, A. H.; Bergman, R. G. Carbon-Hydrogen Activation in Completely Saturated Hydrocarbons: Direct Observation of M + R-H. Fwdarw. M(R)(H). J. Am. Chem. Soc. 1982, 104 (1), 352–354.
- (14) Arndtsen, B. A.; Bergman, R. G.; Mobley, T. A.; Peterson, T. H. Selective Intermolecular Carbon-Hydrogen Bond Activation by Synthetic Metal Complexes in Homogeneous Solution. *Acc. Chem. Res.* 1995, 28 (3), 154–162.
- (15) Jones, W. D.; Feher, F. J. Comparative Reactivities of Hydrocarbon Carbon-Hydrogen Bonds with a Transition-Metal Complex. *Acc. Chem. Res.* **1989**, 22 (3), 91–100.
- (16) Hall, C.; Perutz, R. N. Transition Metal Alkane Complexes †. *Chem. Rev.* **1996**, *96* (8), 3125–3146.
- (17) Niu, S.; Hall, M. B. Theoretical Studies on Reactions of Transition-Metal Complexes. *Chem. Rev.* **2000**, *100* (2), 353–406.
- (18) Balcells, D.; Clot, E.; Eisenstein, O. C—H Bond Activation in Transition Metal Species from a Computational Perspective. *Chem. Rev.* **2010**, *110* (2), 749–823.
- (19) George, M. W.; Hall, M. B.; Portius, P.; Renz, A. L.; Sun, X.-Z.; Towrie, M.; Yang, X. Combined Experimental and Theoretical Investigation into C–H Activation of Cyclic Alkanes by Cp'Rh(CO)2 (Cp'=H5-C5H5 or H5-C5Me5). Dalton Trans. 2011, 40 (8), 1751.
- (20) George, M. W.; Hall, M. B.; Jina, O. S.; Portius, P.; Sun, X.-Z.; Towrie, M.; Wu, H.; Yang, X.; Zaric, S. D. Understanding the Factors Affecting the Activation of Alkane by Cp'Rh(CO)2 (Cp' = Cp or Cp\*). *Proc. Natl. Acad. Sci. U. S. A.* **2010**, *107* (47), 20178–20183.
- (21) Pitts, A. L.; Wriglesworth, A.; Sun, X.-Z.; Calladine, J. A.; Zarić, S. D.; George, M. W.; Hall, M. B. Carbon—Hydrogen Activation of Cycloalkanes by Cyclopentadienylcarbonylrhodium—A Lifetime Enigma. *J. Am. Chem. Soc.* **2014**, *136* (24), 8614—8625.
- (22) Blake, A. J.; George, M. W.; Hall, M. B.; McMaster, J.; Portius, P.; Sun, X. Z.; Towrie, M.; Webster, C. E.; Wilson, C.; Zarić, S. D. Probing the Mechanism of Carbon-Hydrogen Bond Activation by Photochemically Generated Hydridotris(Pyrazolyl)Borato Carbonyl Rhodium Complexes: New Experimental and Theoretical Investigations. *Organometallics* **2008**, 27 (2), 189–201.
- (23) Guan, J.; Wriglesworth, A.; Sun, X. Z.; Brothers, E. N.; Zarić, S. D.; Evans, M. E.; Jones, W. D.; Towrie, M.; Hall, M. B.; George, M. W. Probing the Carbon-Hydrogen Activation of Alkanes Following

Photolysis of Tp' Rh(CNR)(Carbodiimide): A Computational and Time-Resolved Infrared Spectroscopic Study. *J. Am. Chem. Soc.* **2018**, 140 (5), 1842–1854.

- (24) Lian, T.; Bromberg, S. E.; Yang, H.; Proulx, G.; Bergman, R. G.; Harris, C. B. Femtosecond IR Studies of Alkane C-H Bond Activation by Organometallic Compounds: Direct Observation of Reactive Intermediates in Room Temperature Solutions. *J. Am. Chem. Soc.* 1996, 118 (15), 3769–3770.
- (25) Asbury, J. B.; Ghosh, H. N.; Yeston, J. S.; Bergman, R. G.; Lian, T. Sub-Picosecond IR Study of the Reactive Intermediate in an Alkane C-H Bond Activation Reaction by CpRh(CO) <sub>2</sub>. Organometallics 1998, 17 (16), 3417–3419.
- (26) Asbury, J. B.; Hang, K.; Yeston, J. S.; Cordaro, J. G.; Bergman, R. G.; Lian, T. Direct Observation of a Picosecond Alkane C-H Bond Activation Reaction at Iridium. *J. Am. Chem. Soc.* **2000**, *122* (51), 12870–12871.
- (27) Frisch, M. J. et al. *Gaussian 09*, Revision D.01; Gaussian Inc.: Wallingford, CT, 2009.
- (28) Tao, J.; Perdew, J. P.; Staroverov, V. N.; Scuseria, G. E. Climbing the Density Functional Ladder: Nonempirical Meta—Generalized Gradient Approximation Designed for Molecules and Solids. *Phys. Rev. Lett.* **2003**, *91* (14), 146401.
- (29) Peverati, R.; Truhlar, D. G. Improving the Accuracy of Hybrid Meta-GGA Density Functionals by Range Separation. *J. Phys. Chem. Lett.* **2011**, 2 (21), 2810–2817.
- (30) Peverati, R.; Truhlar, D. G. M11-L: A Local Density Functional That Provides Improved Accuracy for Electronic Structure Calculations in Chemistry and Physics. *J. Phys. Chem. Lett.* **2012**, 3 (1), 117–124.
- (31) Peverati, R.; Truhlar, D. G. Screened-Exchange Density Functionals with Broad Accuracy for Chemistry and Solid-State Physics. *Phys. Chem. Chem. Phys.* **2012**, *14* (47), 16187.
- (32) Chai, J.-D.; Head-Gordon, M. Long-Range Corrected Hybrid Density Functionals with Damped Atom—Atom Dispersion Corrections. *Phys. Chem. Chem. Phys.* **2008**, *10* (44), 6615.
- (33) Figgen, D.; Peterson, K. A.; Dolg, M.; Stoll, H. Energy-Consistent Pseudopotentials and Correlation Consistent Basis Sets for the 5d Elements Hf–Pt. *J. Chem. Phys.* **2009**, *130* (16), 164108.
- (34) Dunning, T. H. Gaussian Basis Sets for Use in Correlated Molecular Calculations. I. The Atoms Boron through Neon and Hydrogen. *J. Chem. Phys.* **1989**, *90* (2), 1007–1023.
- (35) Marenich, A. V.; Cramer, C. J.; Truhlar, D. G. Universal Solvation Model Based on Solute Electron Density and on a Continuum Model of the Solvent Defined by the Bulk Dielectric Constant and Atomic Surface Tensions. *J. Phys. Chem. B* **2009**, *113* (18), 6378–6396.
- (36) Costello, J. F.; Davies, S. G.; Gould, E. T. F.; Thomson, J. E. Conformational Analysis of Triphenylphosphine Ligands in Stereogenic Monometallic Complexes: Tools for Predicting the Preferred Configuration of the Triphenylphosphine Rotor. *Dalton Trans.* **2015**, 44 (12), 5451–5466.
- (37) Jones, W. D.; Feher, F. J. Mechanism of Arene Carbon-Hydrogen Bond Activation by (C5MeS)Rh(PMe3)(H)Ph. Evidence for Arene Precoordination. *J. Am. Chem. Soc.* **1982**, *104* (15), 4240–4242.
- (38) Harrison, J. A.; Nielson, A. J.; Sajjad, M. A.; Schwerdtfeger, P. Evaluation of the Agostic and Syndetic Donations in Aromatic Ring Agostic Interactions Involved in Heteroatom Ligand-Directed C–H Bond Activation. *Organometallics* **2019**, 38 (9), 1903–1916.